A Study on the Geoeffectiveness of Halo Coronal Mass Ejections During the Period of 1996-2018

Hemlata Dharmashaktu[1*] • Naval Kishor Lohani[2] • Mukul Tewari[2]

[1] *Department of Physics, IPGGPG College of Commerce, Haldwani*
[2] *Department of Physics, MB Govt PG College Haldwani*

*Corresponding Author Email id: hemlata.dharmashaktu@gmailcom

Received: 02.08.2023; Revised: 13.12.2023; Accepted: 14.12.2023

Abstract: In this study, we investigate the solar origins and interplanetary properties of 83 geoeffective halo coronal mass ejections (CMEs) that produced intense geomagnetic storms (Dst ≤ -100 nT) on Earth, spanning the time interval from 1996 to 2018, which includes solar cycles 23 and 24. Observations indicate that full-halo CMEs are potential contributors to intense geomagnetic activity on Earth. However, it is worth noting that not all full-halo CMEs lead to significant geomagnetic storms, which adds complexity to the task of space weather forecasting. Our investigation delves into the solar origins and flare connections of these geoeffective CMEs and their interplanetary effects, specifically, solar wind speed, and the southward component of the interplanetary magnetic field Bz. The objective is to elucidate the relationship between solar and interplanetary parameters. Specifically, this study aims to identify solar parameters that govern key interplanetary parameters responsible for generating significant geomagnetic storms. Our findings indicate that fast full-halo CMEs, associated with powerful flares and originating from favourable locations (i.e., near the central meridian and at low to mid latitudes), are the most likely candidates for producing intense geomagnetic storms. Additionally, our results demonstrate that the intensity of geomagnetic storms is most strongly influenced by the southward component of the interplanetary magnetic field, but is less dependent on the initial speed of the CME.

Key words: Sun • halo CMEs • Initial speed • Geomagnetic storms

Introduction

Coronal mass ejections are is an expulsion of large quantities of magnetic flux and plasma from the Sun into the interplanetary medium. (Gosling et al., 1991;Gosling 1993; K.E.J. Huttunen et al., 2006,). They possess the potential to impact the heliosphere, interplanetary space, and Earth's atmosphere significantly (Howard et al., 1982; Webb and Howard 2012; Lamy et al., 2019). CMEs that emerge near the solar disk centre have a higher probability of directly impacting Earth, thereby being instrumental in the prediction of geomagnetic storms. This is particularly true for intense geomagnetic storms which are primarily caused by these types of CMEs. A subset of these Earth-facing CMEs, known as Halo CMEs (Jackson and Howard 1993; Yermolaev et al., 2005) demonstrate rapid expansion and give the impression of encircling the occulting disk of the coronagraphic observers. Halo CMEs are categorized into two types: full halos (type F), asymmetric halos (type A) and both type observable (or sky plane) width spans 360^0.The full 'halo CMEs' constitute 3% of all CMEs and tend to originate near the disk centre, albeit roughly 10% emerge near the limb (Gopalswamy et al., 2015a). During a period of 73 months in Solar Cycle 24, which is widely acknowledged as one of the weakest solar cycles on record, an average of 3.56 halo coronal mass ejections (CMEs) per month was observed.

(Makela et al. 2015). Halo CMEs originating on the visible portion of the solar disk are termed 'front-sided' events, while those emerging on the unobservable side are referred to as 'back-sided' events and propagate in an anti-Earthward direction. Generally, A-type halos originate nearer to the solar limb and can be in front of, at, or behind the limb. The capacity of CMEs to trigger geomagnetic storms is described as 'geo-effectiveness'. CMEs that impinge on Earth exert profound influences on both technological systems and human activities (Cannon et al., 2013). The intensity of a CME's impact on the geospace environment is profoundly linked to the macroscopic parameters of the solar wind and its magnetic properties, most notably the interplanetary magnetic field (IMF) B, southward component of interplanetary magnetic field Bz and the solar wind speed etc. These parameters such as density and speed are instrumental in determining the degree of compression the magnetosphere undergoes when impinged upon by the solar wind. Furthermore, a southward orientation of the magnetic field primarily facilitates reconnection at the dayside magnetopause, which in turn promotes the development of intense disturbances in the geomagnetic field. These disturbances are commonly referred to as geomagnetic storms (Gonzalez et al., 1999; Gopalswamy et al., 2010; Lugaz et al., 2016).

Geomagnetic storms can be categorized by their disturbance storm time (Dst) values as weak (-30 to -50 nT), moderate (-50 to -100 nT), strong (-100 to -200 nT), severe (-200 to -350 nT), and great (< -350 nT) (Loewe 1997). Although both CMEs and Corotating Interaction Regions (CIRs) can incite weak and moderate storms, the strong, severe, and great storms are exclusively triggered by CMEs (Gosling et al., 1990). While CIRs can account for approximately 10% of strong storms, the Dst values typically do not plummet below -100 nT (Sheeley et al., 1976; Miyoshi and Kataoka 2005; Zurbuchen and Richardson 2006).

Predominantly, substantial disturbances are elicited by CMEs originating from the solar disk's centre, though events initiated near or at the western limb can provoke moderate disturbances (Huttunen et al., 2002; Kilpua et al., 2014; Cid et al., 2012). Conversely, CMEs instigated at the disk centre can also be deflected from the Sun-Earth trajectory due to non-radial channelling incited by rapid solar wind streams produced by neighbouring coronal holes.

The aim of this study is to conduct a quantitative analysis of CMEs having speed above 500 km/s only and have examined their association of with various classes of solar flares, solar wind parameters and geomagnetic storms measured in terms of Dst index.

Data Analysis

The data for the halo coronal mass ejections were obtained from a catalogue that includes all manually identified CMEs from 1996 onwards. This catalogue is based on observations obtained from the Large Angle and Spectrometric Coronagraph (LASCO) instrument aboard the Solar and Heliospheric Observatory (SOHO) mission (Anonymous 2005; Gopalswamy et al., 2010). This catalogue provides comprehensive information on various characteristics of each CME, including the date and time of its occurrence within Lassos field of view, CME linear speed (LS), acceleration, location, associated solar flare class, and other pertinent information. In our study, we utilized data from both LASCO and the Extreme Ultraviolet Imaging Telescope (EIT) (Artzner et al. 1995) to examine the solar origins of the CMEs. The Extreme Ultraviolet Imaging Telescope (EIT) captures images of the Sun in four different wavelength bands, including one specific band that measures at 195 Angstroms. We used images from the LASCO coronagraphs C2 and C3, which provide a combined field of view ranging from 2 to 30 solar radii, for tracking the CMEs in the outer corona. The time at which the initial brightening was observed in the EIT images was deemed to be the initiation point of the flare or CME activity. We follow a criterion similar to that of (Y. M. Wang et al., 2002; Srivastava and Venkatakrishnan 2004) to determine the solar source of a geomagnetic storm. For the purpose of this study, we have selected a temporal window of 1 to 5 days prior to the occurrence of the storm.

Furthermore, we acquired data on the total magnetic field and the southward component of the interplanetary magnetic field (IMF), which are vital for understanding the development of intense storms, solar wind parameters, and the disturbance storm time (Dst). This data was collected from the Omniweb data centre, which is available at https://omniweb.gsfc.nasa.gov/form/dx1.html.

Our analysis identified 83 halo CMEs with speeds greater than 500 km/s and associated with 68 intense geomagnetic storms events with a Dst index ≤-100 nT.

Results and Discussion

Variations in geomagnetic storms during the solar cycle 23 and 24: Figure 1 illustrates the year-wise variation of the number of halo coronal mass ejections (CMEs) associated with geomagnetic storms (GMS), GMS with a Dst index ≤ -100 nT, and sunspot numbers between 1996 and 2018. The data clearly indicates an increase in the number of halo CMEs from solar minimum to solar maximum, following the sunspot cycle. This suggests that CMEs are part of a class of solar active phenomena. During this time period, a total of 101 intense geomagnetic storms were recorded, with 66 associated with halo CMEs. Therefore, we have excluded from our study any geomagnetic storms not linked with halo CMEs. Our investigation is thus focused on the solar sources of the remaining 66 geomagnetic storms. In 1996, during the solar minimum, no geomagnetic storms were recorded, compared to 12 geomagnetic storms near the solar maximum in 2001. The number of intense geomagnetic storms during our study period increased from one in 1997 to 10 in 2000, reflecting an increase in line with the progression of solar activity. There was a notable decrease in the frequency of geomagnetic storms since 1999, with the number of events reducing from three in 1998 to just one in 1999.

Moreover, 15 super intense storms (Dst ≤ -200 nT) occurred during solar cycle 23, whereas only 3 happened in solar cycle 24, with the highest number, 5, occurring in the year 2004. The year 1999 is noteworthy for its decline in overall geomagnetic storms, including super intense events, which aligns with the overall reduction in solar and related interplanetary activity that year (Manoharan et al. 2004). The temporary decrease in the frequency of geomagnetic storms has been attributed to the restructuring of the near-ecliptic solar wind (Richardson and Cane 2011). The occurrence rate of GMEs in solar cycle 23 was 3.7 times higher than in solar cycle 24. The diminished number of intense GMS in solar cycle 24 is indicative of a weak solar cycle (Kilpua et al., 2014).

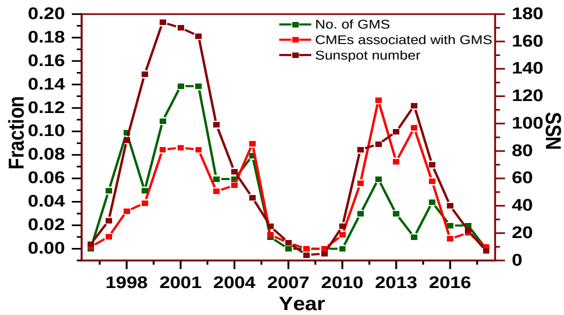

Figure1. Year wise variation of fraction of GMS (Dst ≤ -100nT), fraction of halo CMEs associated with GMS and yearly average of sunspot number

Location of Solar Sources of halo CMEs:

The location of the origin of halo CMEs seems to be significant factor in determining their geo-effectiveness. Previous research has suggested that halo CMEs originating from the front side of the solar disk may have a geoeffective on Earth, provided that that they originate from favourable locations, specifically, within the vicinity of the central meridian and at lower latitudinal regions (Gonzalez et al.,1999; T. Wang et al., 2002; Srivastava and Venkatakrishnan 2002, 2004) . Our present analysis we examine the locations of 80 halo CMEs and their association with solar flares. The spatial distribution of location of halo CMEs across the solar disk is depicted in Fig.2. There is a significant longitudinal asymmetry in the distribution of source regions of geoeffective

CMEs, and they are more likely to originate from the western hemisphere than from the eastern hemisphere. Nearly 65% of them originated from the west of the central meridian, whereas approximately 32% appear from the east side. The skewed distribution is in in agreement with the findings of (T. Wang et al., 2002; Verma et al., 2020), however, this is in contrast to the findings of (Cane and Richardson 2003; Srivastava and Venkatakrishnan 2004), who found that CMEs with Earth-impacting halos have an approximately even distribution in longitude. Figure 1 illustrates this point: approximately 97% of the events occurred within ±30° of the equatorial plane, while about ~73% were primarily concentrated within $\pm 40^0$ of the solar longitude. The findings are in agreement with the results of (Gopalswamy et al., 2010)which revealed that 70% of the events occur within a range of ±30° solar longitudes. Interestingly, no clear preference for either the northern or southern hemisphere was observed among halo CMEs impacting the Earth, aligning with the findings of (Cane and Richardson 2003) and (Y. M. Wang et al., 2002). Our study found that 32 events emanated from the northern hemisphere, compared to 42 from the southern hemisphere. Consequently, from our analysis of the origins of all the geo-effective CMEs are usually found in the active region belt, which is usually found near the central meridian and at low and middle latitudes

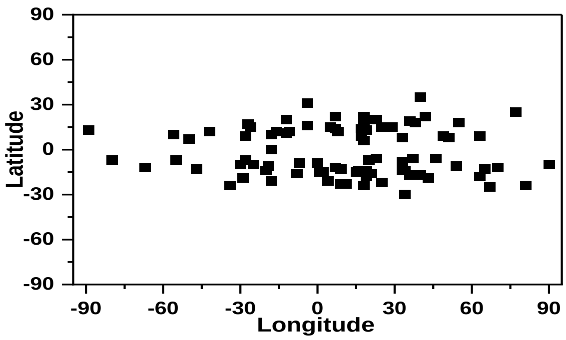

Figure 2. The location of the solar sources of the geoeffective CMEs during 1996–2018.

Fig.3 shows that the plot between the solar flare class and the fraction of halo CMEs. Our observations revealed that halo CMEs displayed varying associations with different flare classes: 1 (1%) were associated with class B flares, 18 (22%) with class C flares, 33 (40%) with class M flares, and 31 (37%) with class X flares. Furthermore, it has been observed that 85% of geoeffective halo CMEs are associated with solar flares, and M class flare events are the predominant ones. Our findings are in agreement with the earlier findings of (Verma et al., 2020).

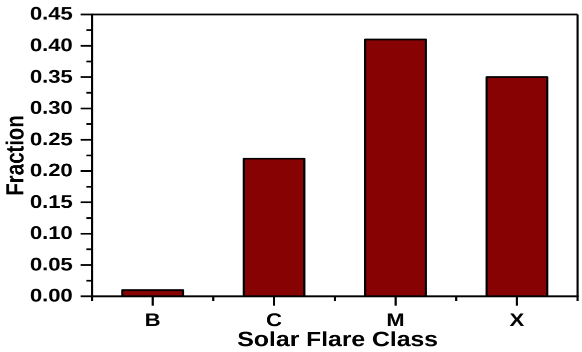

Figure 3. Fraction of halo CMEs associated with different class of solar flares.

Initial Speeds of the Geoeffective CMEs and Solar wind Parameters: The determination of the linear speed of CMEs is one of the most challenging parameters that can be extracted from coronagraphic images. The radial speed of Earth-directed halo CMEs cannot be directly measured due to the unfavourable observational positioning from Earth. Recent data from the Large Angle and Spectrometric Coronagraph (LASCO) suggests that CMEs exhibit certain unique features regardless of their trajectory. One such attribute is the consistency in the geometric shape of the expelled matter, which is preserved throughout the LASCO coronagraphs' field of vision (Chen et al., 2012). This observation implies a proportional relationship between radial propagation and the lateral expansion of the clouds. Hence, the radial speed of halo CMEs can be deduced from the speed of

 DOI: https://doi.org/10.51220/jmr.v18i2.16

their lateral expansion. Using LASCO imagery, it's feasible to estimate propagation speed up to 30 solar radii. For distances beyond this, near-Earth in situ measurements can be applied.

During 1996-2018, the initial speeds of 82% of halo CMEs observed were greater than 500 km/s. In Solar Cycle 23, the speed ranges from 65 to 3387 km/s (Manoharan et al., 2004; Mittal and Narain 2009) whereas during Solar Cycle 24, it ranges from 113 to 3163 km/s. The initial velocity of geoeffective halo CMEs was observed to be within the range of 500-2700 km/s. We observed a correlation coefficient -0.23 between CMEs initial speed and Dst index with 95% of confidence level (Fig.4).

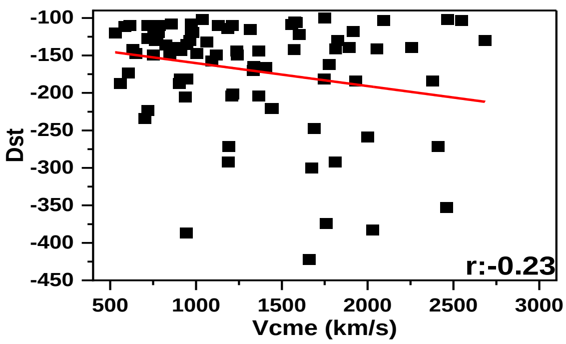

Figure 4. Plot of initial speed of halo CMEs with Dst index.

Our findings were inconsistent with previous studies. In 2002, Srivastava and Venkatakrishnan reported a high correlation coefficient of 0.83 when they considered only the initial speed of geoeffective CMEs associated with intensive X-class events. Meanwhile, Nandita and Venkatakrishnan in 2004 observed a significant correlation of approximately 0.66 between the initial speed of the CMEs and the Dst index. Their method of calculating the correlation coefficient excluded high-speed CMEs associated with low Dst values, such as the event that occurred on April 18, 2001. During this event, a limb halo CME with an initial speed of 2400 km/s resulted in an intense geomagnetic storm with a Dst index of -103 nT. In contrast, (Mittal and Narain 2015), found a negligible correlation between the initial speed of halo CMEs and the Dst index. Yet (Dumbović et al. 2015) said that faster CMEs are more likely to cause strong geomagnetic storms. Furthermore, he found that slow CMEs (600 km/s) are unlikely to cause intense storms (|Dst| > 200 nT) unless they are in an interaction with a faster CME. However, it is important to note that a single parameter, such as its initial speed, does not determine the geoeffectiveness of CMEs, but we cannot ignore the importance of the initial speed of CME as geoeffective parameter.

Interplanetary Sources of Intense Geomagnetic Storms: Previous research, such as the studies conducted by (Burton et al. 1975)and (Gonzalez et al. 1989), noted that the geoeffectiveness of solar wind is contingent on its speed and the embedded southward component of the interplanetary magnetic field (IMF). A southward-oriented IMF is more geoeffective compared to its northward counterpart. The intensity of a geomagnetic storm is determined by the interaction between the solar wind plasma and the orientation of the magnetic field. Specifically, the IMF B plays a pivotal role in generating geomagnetic storms, especially when the southward IMF Bz and geomagnetic field lines are oriented in an antiparallel fashion, enabling magnetic reconnection. The strongest magnetospheric coupling occurs when the IMF Bz component is oriented southward (Gonzalez et al. 1989). An enhanced ring current serves as the primary indicator of a magnetic storm. The magnitude of a geomagnetic storm is measured by the disturbance storm time (Dst) index.

Our findings reveal a Pearson's correlation coefficient of 0.69 between the Dst values and the minimum southward component of the IMF Bz at a 95% confidence level (Figure 5a). Additionally, the fluctuation of Bz plays a crucial role in determining the amount of solar wind energy transferred to the magnetosphere (Gonzalez et al. 1999). The most substantial decrease in Bz causes the most significant reduction in Dst, supporting our prior assertion that Bz is an effective parameter for producing

DOI: https://doi.org/10.51220/jmr.v18i2.16

geomagnetic storms (Rathore, Gupta, and Kaushik, 2015; (Pokharia et al. 2017). Furthermore, we also analyzed the correlation between geomagnetic storm intensity and BzV to further explore the solar wind-magnetosphere coupling mechanism. This analysis helps to enhance our understanding of the energization mechanisms of these storms.

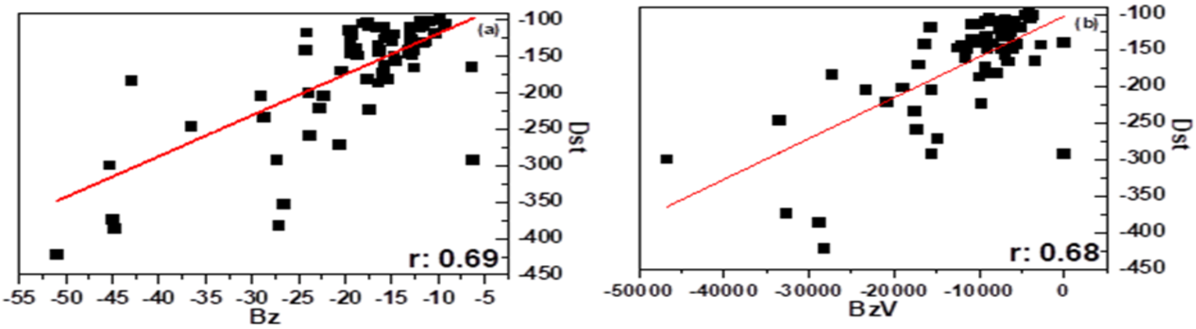

Figure 5. Plot shows the variation Bz and BzV with Dst index.

Figure 5b, depicts the dependence of Dst on BzV, exhibiting a good correlation of 0.68 at a 95% confidence level. The high correlation of Bz and BzV with the Dst suggests that both Bz and BzV are good indicators for predicting geomagnetic storm occurrences.

Conclusion

As part of the present work, we have studied several observational characteristics of halo CMEs during solar cycles 23 and 24 from 1996 to 2018. The following are some of the most important conclusions from this statistical analysis.

1) 66 out of 101 intense GMSs (Dst ≤ -100nT) were associated with halo CMEs with initial speed greater than 500 km/s.
2) 83% of super intense GMSs belongs to solar cycle 23.
3) There is a significant longitudinal asymmetry in the distribution of source regions of geoeffective CMEs, and 65% likely to originate from the western hemisphere whereas 32% from eastern hemisphere.
4) 85% geoeffective halo CMEs were associated with solar flares.
5) Low correlation 0.23 shows between CME initial speed and Dst index.
6) High correlation shows between southward component of IMF (Bz) and BzV and Dst 0.69 and 0.68 respectively.

Acknowledgement

Authors would like to thank an anonymous referee for providing fruitful comments and suggestions on the paper. The authors greatly acknowledge the data support provided by SOHO/LASCO CME catalogue and Omni web Centre. We are thankful to our college authorities for their help and encouragement.

References

Anonymous. 2005. “The Last Word: The Definition of Halo Coronal Mass Ejections.” *Eos, Transactions American Geophysical Union* 86(30):281.

Artzner, G. E., J. Brunaud, A. H. Gabriel, J. F. Hochedez, X. Y. Song, B. Au, K. P. Dere, R. A. Howard, R. Kreplin, J. D. Moses, J. M. Defise, Centre Spatial De Liege, R. C. Catura, J. R. Lemen, L. Siting, R. A. Stern, Lockheed Palo, Palo Alto, and W. M. Neupert. 1995. “Imaging Telescope.” 291–312.

Burton, R. K., R. L. McPherron, and C. T. Russell. 1975. “An Empirical Relationship between Interplanetary Conditions and Dst .” *Journal of Geophysical Research* 80(31):4204–14.

Cane, H. V. and I. G. Richardson. 2003. "Interplanetary Coronal Mass Ejections in the Near-Earth Solar Wind during 1996-2002." *Journal of Geophysical Research: Space Physics* 108(A4).

Chen, Guang Ming, Jiyao Xu, Wenbin Wang, Jiuhou Lei, and Alan G. Burns. 2012. "A Comparison of the Effects of CIR-and CME-Induced Geomagnetic Activity on Thermospheric Densities and Spacecraft Orbits: Case Studies." *Journal of Geophysical Research: Space Physics* 117(8).

Cid, C., H. Cremades, A. Aran, C. Mandrini, B. Sanahuja, B. Schmieder, M. Menvielle, L. Rodriguez, E. Saiz, Y. Cerrato, S. Dasso, C. Jacobs, C. Lathuillere, and A. Zhukov. 2012. "Can a Halo CME from the Limb Be Geoeffective?" *Journal of Geophysical Research: Space Physics* 117(11).

Dumbović, M., A. Devos, B. Vršnak, D. Sudar, L. Rodriguez, D. Ruždjak, K. Leer, S. Vennerstrøm, and A. Veronig. 2015. "Geoeffectiveness of Coronal Mass Ejections in the SOHO Era." *Solar Physics* 290(2):579–612.

Gonzalez, Walter D., Bruce T. Tsurutani, and Alicia L. Clúa De Gonzalez. 1999. "Interplanetary Origin of Geomagnetic Storms." *Space Science Reviews* 88(3–4):529–62.

Gonzalez, Walter D., Bruce T. Tsurutani, Alicia L. C. Gonzalez, Edward J. Smith, Frances Tang, and Syun-I. Akasofu. 1989. "Solar Wind-Magnetosphere Coupling during Intense Magnetic Storms (1978-1979)." *J of Geophysical Research* 94(A7):8835.

Gopalswamy, Nat, Seiji Yashiro, Hong Xie, Sachiko Akiyama, and Pertti Mäkelä. 2010. "Large Geomagnetic Storms Associated with Limb Halo Coronal Mass Ejections." *Advances in Geosciences: Volume 21: Solar Terrestrial (ST)* (April):71–82.

Gosling, J. T. 1993. "The Solar Flare Myth." *Journal of Geophysical Research: Space Physics* 98(A11):18937–49.

Gosling, J. T., S. Bame, D. J. Mccomas, and L. Phillips. 1990. "Large from Bow Presentation Alamos Plasma Experiment Events and in Which Kp Was." 17(7):901–4.

Gosling, J. T., D. J. McComas, J. L. Phillips, and S. J. Bame. 1991. "Geomagnetic Activity Associated with Earth Passage of Interplanetary Shock Disturbances and Coronal Mass Ejections." *Journal of Geophysical Research* 96(A5):7831.

Howard, Alan D., James A. Cutts, and Karl R. Blasius. 1982. "Stratigraphic Relationships within Martian Polar Cap Deposits." *Icarus* 50(2):161–215.

Huttunen, K. E. J., H. E. J. Koskinen, A. Karinen, and K. Mursula. 2006. "Asymmetric Development of Magnetospheric Storms during Magnetic Clouds and Sheath Regions." *Geophysical Research Letters* 33(6):2–5.

Huttunen, K. Emilia J., Hannu E. J. Koskinen, Tuija I. Pulkkinen, Antti Pulkkinen, Minna Palmroth, E. Geoffrey D. Reeves, and Howard J. Singer. 2002. "April 2000 Magnetic Storm: Solar Wind Driver and Magnetospheric Response." *Journal of Geophysical Research: Space Physics* 107(A12):1–21.

Jackson, Bernard V. and Russ A. Howard. 1993. "A CME Mass Distribution Derived from SOLWIND Coronagraph Observations." *Solar Physics* 148(2):359–70.

Kilpua, E. K. J., M. Mierla, A. N. Zhukov, L. Rodriguez, A. Vourlidas, and B. Wood. 2014. "Solar Sources of Interplanetary Coronal Mass Ejections During the Solar Cycle 23/24 Minimum." *Solar Physics* 289(10):3773–97.

Lamy, P. L., O. Floyd, B. Boclet, J. Wojak, H. Gilardy, and T. Barlyaeva. 2019. "Coronal Mass Ejections over Solar Cycles 23 and 24." *Space Science Reviews* 215(5).

Loewe, C. A. 1997. "Classification and Mean Behavior of Magnetic Storms." *Journal of Geophysical Research: Space Physics*

DOI: https://doi.org/10.51220/jmr.v18i2.16

102(A7):14209–13.

Lugaz, N., C. J. Farrugia, R. M. Winslow, N. Al-Haddad, E. K. J. Kilpua, and P. Riley. 2016. "Factors Affecting the Geoeffectiveness of Shocks and Sheaths at 1 AU." *Journal of Geophysical Research: Space Physics* 121(11):10,861-10,879.

Makela, P., N. Gopalswamy, S. Akiyama, H. Xie, and S. Yashiro. 2015. "Estimating the height of CMEs associated with a major SEP event at the onset of the metric type II radio burst during solar cycles 23 and 24." *Astrophysical Journal* 806(1).

Manoharan, P. K., N. Gopalswamy, S. Yashiro, A. Lara, G. Michalek, and R. A. Howard. 2004. "Influence of Coronal Mass Ejection Interaction on Propagation of Interplanetary Shocks." *Journal of Geophysical Research: Space Physics* 109(A6).

Mittal, Nishant and Udit Narain. 2009. "On Some Properties of Coronal Mass Ejections in Solar Cycle 23." *New Astronomy* 14(3):341–46.

Mittal, Nishant and Udit Narain. 2015. "On the Arrival Times of Halo Coronal Mass Ejections in the Vicinity of the Earth." *NRIAG Journal of Astronomy and Geophysics* 4(1):100–105.

Miyoshi, Yoshizumi and Ryuho Kataoka. 2005. "Ring Current Ions and Radiation Belt Electrons during Geomagnetic Storms Driven by Coronal Mass Ejections and Corotating Interaction Regions." *Geophysical Research Letters* 32(21):1–5.

Pokharia, Meena, Lalan Prasad, Chandni Mathpal, Chandrasekhar Bhoj, Hema Kharayat, and Rajesh Mathpal. 2017. "Association Between the Solar Wind Speed, Interplanetary Magnetic Field and the Cosmic Ray Intensity for Solar Cycles 23 and 24." *Journal of Astrophysics and Astronomy* 38(4):1–9.

Richardson, I. G. and H. V. Cane. 2011. "Geoeffectiveness (Dst and Kp) of Interplanetary Coronal Mass Ejections during 1995-2009 and Implications for Storm Forecasting." *Space Weather* 9(7):1-9.

Sheeley, N. R., J. W. Harvey, and W. C. Feldman. 1976. "Coronal Holes, Solar Wind Streams, and Recurrent Geomagnetic Disturbances: 1973-1976." *Solar Physics* 49(2):271–78.

Srivastava, Nandita and P. Venkatakrishnan. 2004. "Solar and Interplanetary Sources of Major Geomagnetic Storms during 1996-Solar and Interplanetary Sources of Major." (July 2014).

Verma, Virendra Kumar, Nishant Mittal, and Ramesh Chandra. 2020. "Some Kinematics of Halo Coronal Mass Ejections." *Open Astronomy* 29(1):81–88.

Wang, Tongjiang, Yihua Yan, Jialong Wang, H. Kurokawa, and K. Shibata. 2002. "The Large-Scale Coronal Field Structure and Source Region Features for a Halo Coronal Mass Ejection." *The Astrophysical Journal* 572(1):580–97.

Wang, Y. M., P. Z. Ye, S. Wang, G. P. Zhou, and J. X. Wang. 2002. "A Statistical Study on the Geoeffectiveness of Earth-Directed Coronal Mass Ejections from March 1997 to December 2000." *Journal of Geophysical Research: Space Physics* 107(A11):1–9.

Webb, David F. and Timothy A. Howard. 2012. "Coronal Mass Ejections : Observations Imprint / Terms of Use." *Living Reviews in Solar Physics* 9(3).

Yermolaev, Yu I., M. Yu Yermolaev, G. N. Zastenker, L. M. Zelenyi, A. A. Petrukovich, and J. A. Sauvaud. 2005. "Statistical Studies of Geomagnetic Storm Dependencies on Solar and Interplanetary Events: A Review." *Planetary and Space Science* 53(1–3):189–96.

Zurbuchen, Thomas H. and Ian G. Richardson. 2006. "In-Situ Solar Wind and Magnetic Field Signatures of Interplanetary Coronal Mass Ejections." *Space Science Reviews* 123(1–3):31–43.

******